Clean Energy, 2021, 713–730

https://doi.org/10.1093/ce/zkab041
Homepage: https://academic.oup.com/ce

Research Article

Modelling and reviewing the reliability and multi-objective optimization of wind-turbine system and photovoltaic panel with intelligent algorithms

Reza Alayi[1,*], Mehdi Jahangiri[2], John William Grimaldo Guerrero[3], Ravil Akhmadeev[4], Rustem Adamovich Shichiyakh[5] and Sara Abbasi Zanghaneh[6]

[1]Department of Mechanics, Germi Branch, Islamic Azad University, Germi, Iran
[2]Department of Mechanical Engineering, Shahrekord Branch, Islamic Azad University, Shahrekord, Iran
[3]Departamento de Energía, Universidad de la Costa, Barranquilla, Colombia
[4]Plekhanov Russian University of Economics, Stremyanny lane, 36, Moscow, 117997, Russian Federation
[5]Department of Management, Candidate of Economic Sciences, Kuban State Agrarian University named after I.T. Trubilin, Krasnodar, Russian Federation
[6]Department of Energy Engineering, Energy Institute of Higher Education, Saveh, Iran

*Corresponding author. E-mail: reza.alayi@yahoo.com, reza_alayi@iaugermi.ac.ir

Abstract

One of the options for non-dependence on fossil fuels is the use of renewable energy, which has not grown significantly due to the variable nature of this type of energy. The combined use of wind and solar energy as energy sources can be a good solution to the problem of variable energy output. Therefore, the purpose of this research is to model a combination of the wind-turbine system and photovoltaic cell, which is needed to investigate their ability to supply electrical energy. To determine this important power production, real data of solar-radiation intensity and wind are used and, in modelling photovoltaic cells, the effects of ambient temperature are also considered. In order to generalize the studied system in all dimensions, different scenarios have been considered. According to the amount of electrical power generated, during the evaluation of these scenarios, two economic parameters, namely the selected scenario of a wind/solar system with diesel-generator support, was determined.

Received: 26 May 2021; **Accepted:** 6 September 2021

Graphical Abstract

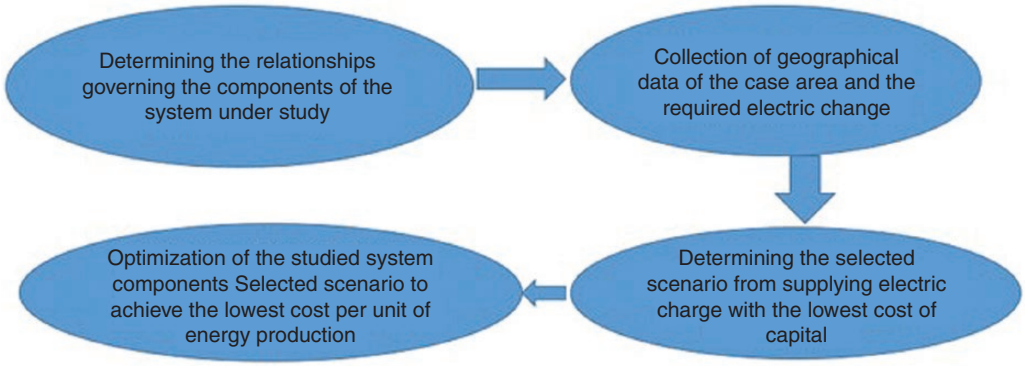

Keywords: reliability; wind turbine; photovoltaic cell; intelligent algorithm; economic analysis

Introduction

Recent years have seen a significant increase in the use of renewable energy sources. In particular, wind and solar energy, which are infinitely location-dependent, non-polluting and sources with high potential for combining and variable energy production [1–3]. For stand-alone and remote systems, such as radio communication systems and satellite ground stations far from power grids, on-site power-generation systems are preferred [4–7]. These systems are usually equipped with diesel generators to deal with peak loads during short periods when available energy is low. Renewable-energy-based hybrid energy systems are the best option to reduce dependence on fossil fuels, one of which is the hybrid wind-turbine and cellular photovoltaic system, which are accessible using wind speed and solar radiation [8–11]. For power generation in grid-independent hybrid systems, several factors must be considered, including power-generation reliability and current costs. It can be emphasized that stand-alone hybrid power-generation systems are more reliable and less expensive than systems that rely on one energy source. Various studies have shown that the use of renewable hybrid energy systems in off-grid applications, especially in remote areas, is economical [12–15]. There are several ways to optimize hybrid systems; these methods include imperialist competitive, ant-colony, genetic algorithms and more [16]. Table 1 shows some recent work done in the field of modelling and optimization using different algorithms.

In addition, climatic conditions can make one type of hybrid system more useful than another. For example, photovoltaic–diesel hybrid systems are ideal in hot regions. In this research, unlike in previous research, different scenarios have been evaluated. In evaluating the scenarios, two economic parameters and the reliability of weighted indicators have been considered for selection. Then the optimization is done with different algorithms. This research has been done with the aim of determining the optimal size of the system consisting of a wind turbine and photovoltaic cell with diesel-generator support and battery storage. To achieve this goal, different scenarios have been considered and determining the size of different technologies with the two goals of access to provide the maximum required electrical load with the lowest cost is considered. In this regard, the colonial-competition algorithm has been used.

1 Materials and methods

1.1 Modelling the studied system

The schematic of the studied system can be seen in Fig. 1. This system includes photovoltaic panels and/or wind turbines and/or diesel generators and/or batteries. The model used in this research is presented for the optimal design of the hybrid system under study based on meteorological data that are sampled and recorded on a daily average. MATLAB software has been used to model the studied system.

1.1.1 *Photovoltaic-cell modelling*

In a photovoltaic cell, the relationship between current and voltage is as follows [25–28]:

$$I = I_{SC} - I_O\left[\exp\left(\frac{Q\,(V + I.R_S)}{KT}\right) - 1\right] - \left(\frac{V + I.R_S}{R_P}\right) \quad (1)$$

When the cells are connected in series, the current is the same for all of them and, for each amount of current, the voltage of a module is determined as follows:

$$V_{module} = n(V_d - I.R_S) \quad (2)$$

The power obtained from the values of I_{sc} and V_{oc} is called the ideal power of the cell. The useful power of a cell is the maximum area of the largest rectangle that can be constructed under the I–V curve. We show the voltage and current related to this mode as I_R and V_R. The maximum useful power will be equal to $I_R \times V_R$. The ratio of the maximum useful power to the ideal power is called the Fill Factor:

$$FF = \frac{I_R.V_R}{V_{OC}.I_{SC}} \quad (3)$$

Table 1: Recent studies on the modelling/optimization of renewable energy

Method	Connection mode	Purpose	Location	Reference, year
MOPSO	On-grid	Study of reliability, cost and environmental impact	Egypt	[17], 2020
Homer	On-grid	Peak-demand reduction	Iran	[18], 2020
Modelling	Off-grid	Providing reliable power	China Mainland	[19], 2020
MOEA/DADE	Off-grid	Study of a reliable and economical inductor	China Mainland	[20], 2020
ANN	Off-grid	Size of a photovoltaic system	Australia	[21], 2021
Homer	Off-grid	Supplying electricity to a remote district	Iran	[22], 2021
MCDM	Off-grid	Techno-economical analysis	Malaysia	[23], 2021
Machine-learning technique	On-grid	Minimization of energy bought from the utility grid, maximization of the state of charge of the battery bank and reduction in carbon-dioxide emissions	Taiwan, China	[24], 2021

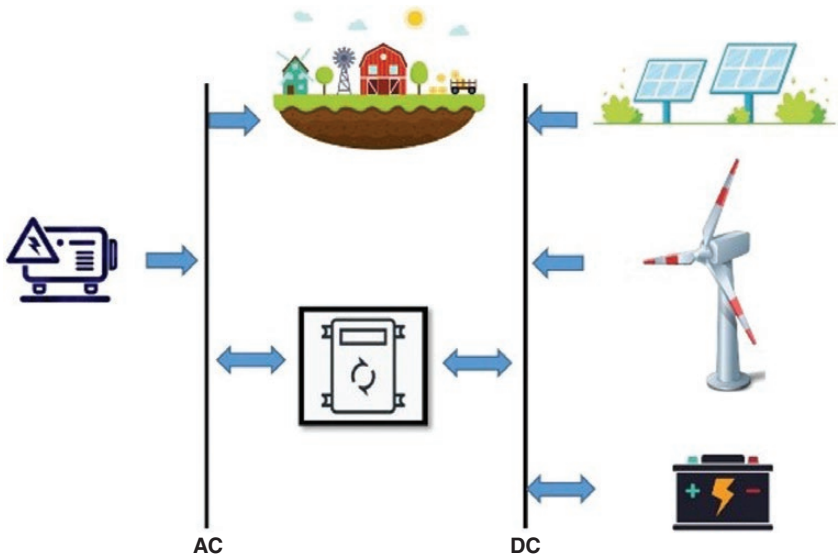

Fig 1: Schematic of the proposed hybrid system.

For silicon cells, the common values of the open-circuit voltage parameters are 450–600 mV, the short-circuit current is 30–50 mA/cm^2 and the Fill Factor is 0.65–0.8. Considering the size of the sample, a cell with an area of 100 cm^2 will be able to generate power of ~61 W. Overall efficiency in a photovoltaic cell is defined as the ratio of power generated to the total input power:

$$t = \frac{I_R.V_R}{P_m} \tag{4}$$

where I_R and V_R are the current and the voltage at the maximum power point. The input power is equal to:

$$P_m = A\int_0^\infty F(\lambda)\left(\frac{hc}{\lambda}\right)d\lambda \tag{5}$$

where A is the cross-sectional area of a cell, $F(\lambda)$ is the number of photons that strike the cell per cubic centimetre per second per unit bandwidth λ, $E = h.c/\lambda$ is the energy of each photon, h is the Planck constant (6.625×10^{-4} $j.s$), c is light speed $\left(3 \times \frac{10^8 m}{s}\right)$, λ is the wavelength in metres and E is in joules. The output power is equal to:

$$P_{out} = I_R \times V_R = FF \times V_{oc} \times I_{sc} \tag{6}$$

It should be noted that at a constant voltage, the current will vary according to the amount of sunlight and therefore the efficiency will also vary according to this issue.

1.1.2 *Wind-turbine modelling*

The mechanical output power at a given wind speed is essentially affected by the turbine speed ratio (TSR), which is defined as the ratio of the turbine rotor speed to the wind speed. At a given wind speed, the maximum turbine energy-conversion efficiency occurs in the optimal TSR. Therefore, as the wind speed changes, the speed of the turbine rotor must also change accordingly to eliminate the optimal TSR and thus extract the maximum energy from available wind sources. The expression for aerodynamic power (P_a) obtained using a wind turbine is obtained by the non-linear expression [29–32]:

$$P_a = 0.5C_p(\lambda)_{p\pi}R^2V_1^3 \tag{7}$$

where P_a is the air density (kg/m^3), R is the rotor radius (m), V_1 is the wind speed (m/s) and C_p is the power factor obtained from the following equation:

$$C_p = (0.44 - 0.0167\beta)\,Sin\left[\frac{\pi(\lambda - 3)}{15.0.3\beta}\right] - 0.00184(\lambda - 3)\beta \quad (8)$$

where β is the angle of inclination of the wind-turbine blade and λ represents TSR, which is obtained from the following relation:

$$\lambda = \frac{\omega_t R}{V_1} \quad (9)$$

where ω is the rotational speed of the blades.

$$\lambda_{opt} = \left[\frac{15 - 0.3\beta}{\pi}\right]\cos^{-1}\left[\frac{0.00184\beta\,(15 - 0.3\beta)}{\pi\,(0.44 - 0.167\beta)}\right] + 3 \quad (10)$$

Therefore, the maximum wind power is obtained from the following equation:

$$P_{a(max)} = 0.5C_{p(max)}(\lambda_{opt}, \beta)\rho\pi R^2 V^3 \quad (11)$$

1.1.3 *Battery model*

In general, changes in battery capacity can be expressed using the temperature coefficient δ_C [33, 34]:

$$C'_{bat} = C_{bat}.\,(1 + \delta_c.\,(T_{bat} - 298.15)) \quad (12)$$

where C'_{bat} is the available or operational capacity of the battery when the battery temperature is $A\ h\ T_{bat}$. The temperature coefficient, δ_C = 6%, is usually used in degrees, otherwise it is determined by the manufacturer. To correctly determine the true state of charge (SOC) of a battery, knowing the initial SOC and current charging or discharging time is essential. However, most storage systems are not ideal and losses occur during charging and discharging as well as during storage periods. These factors are taken into account. Battery SOC at time t + 1 can be easily calculated by:

Fig. 2: Geographical location of the study area.

Source: https://www.google.com/maps.

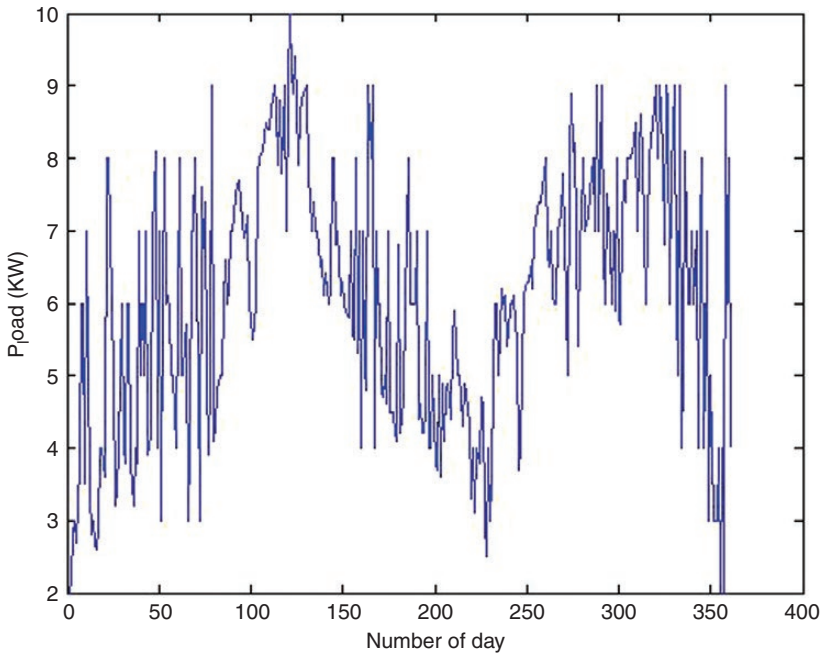

Fig. 3: Average daily required power consumption [17].

$$SOC\,(t+1) = SOC_{(t)}.\left(1 - \frac{\delta.\,\Delta\,t}{24}\right) + \frac{I_{bat}\,(t)\,.\,\Delta\,t.\eta_{bat}}{C'_{bat}} \quad (13)$$

where σ is the self-discharge rate depending on the total charge and battery health and the recommended amount of 0.2% per day; it is difficult to measure the separate charge and discharge efficiencies, so manufacturers usually set a certain efficiency limit. Usually, the battery-charge efficiency is equal to the somewhat adjusted efficiency and the discharge efficiency is 1. The amount of battery current at time t in the hybrid solar–wind system can be described by:

$$I_{bat}(t) = \frac{P_{pv}\,(t) + P_{wt}\,(t) + \frac{P_{AC\ load}(t)}{\eta_i nverter} - P_{DC\ load}(t)}{V_{bat}(t)} \quad (14)$$

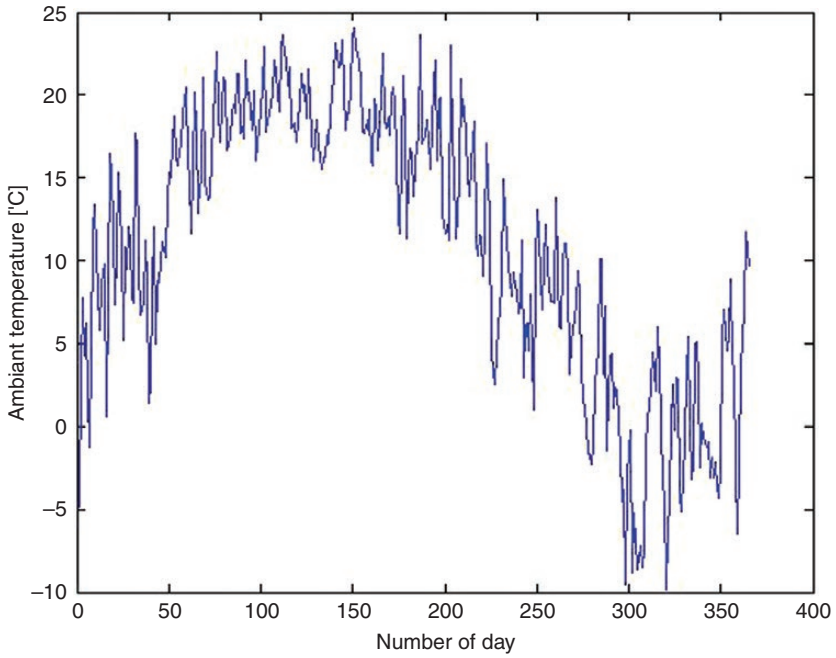

Fig. 4: Average daily ambient temperature.

Source: http://www.satba.gov.ir/.

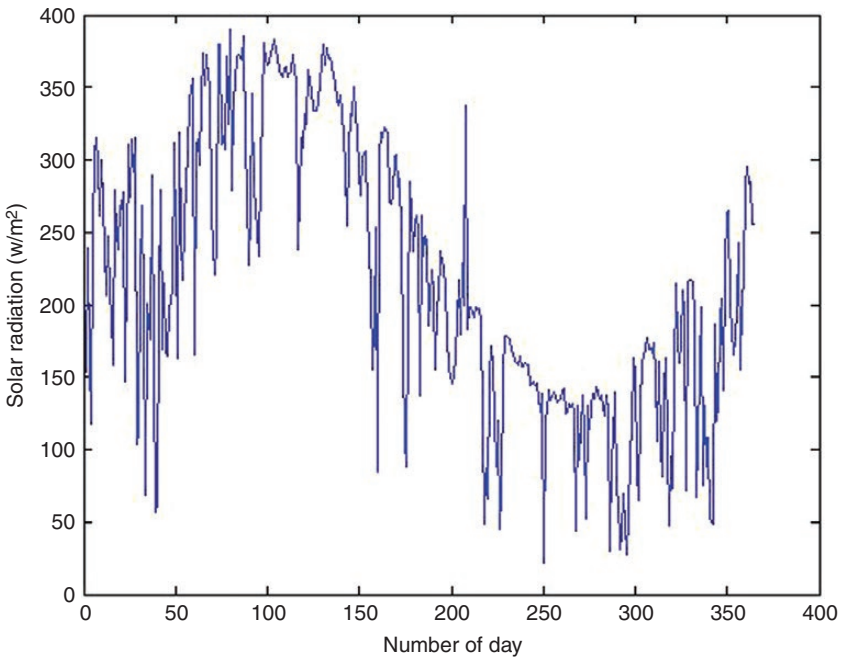

Fig. 5: Average daily intensity of solar radiation.

Source: http://www.satba.gov.ir/.

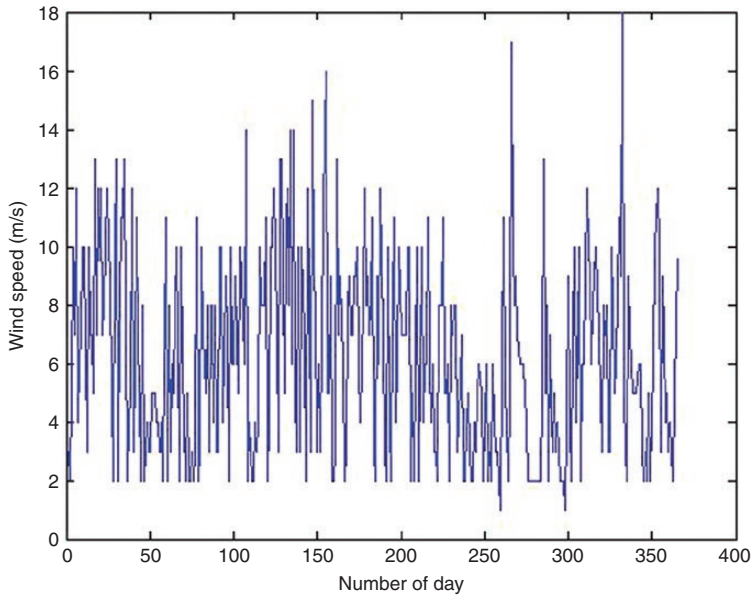

Fig. 6: Average daily wind speed.

Source: http://www.satba.gov.ir/.

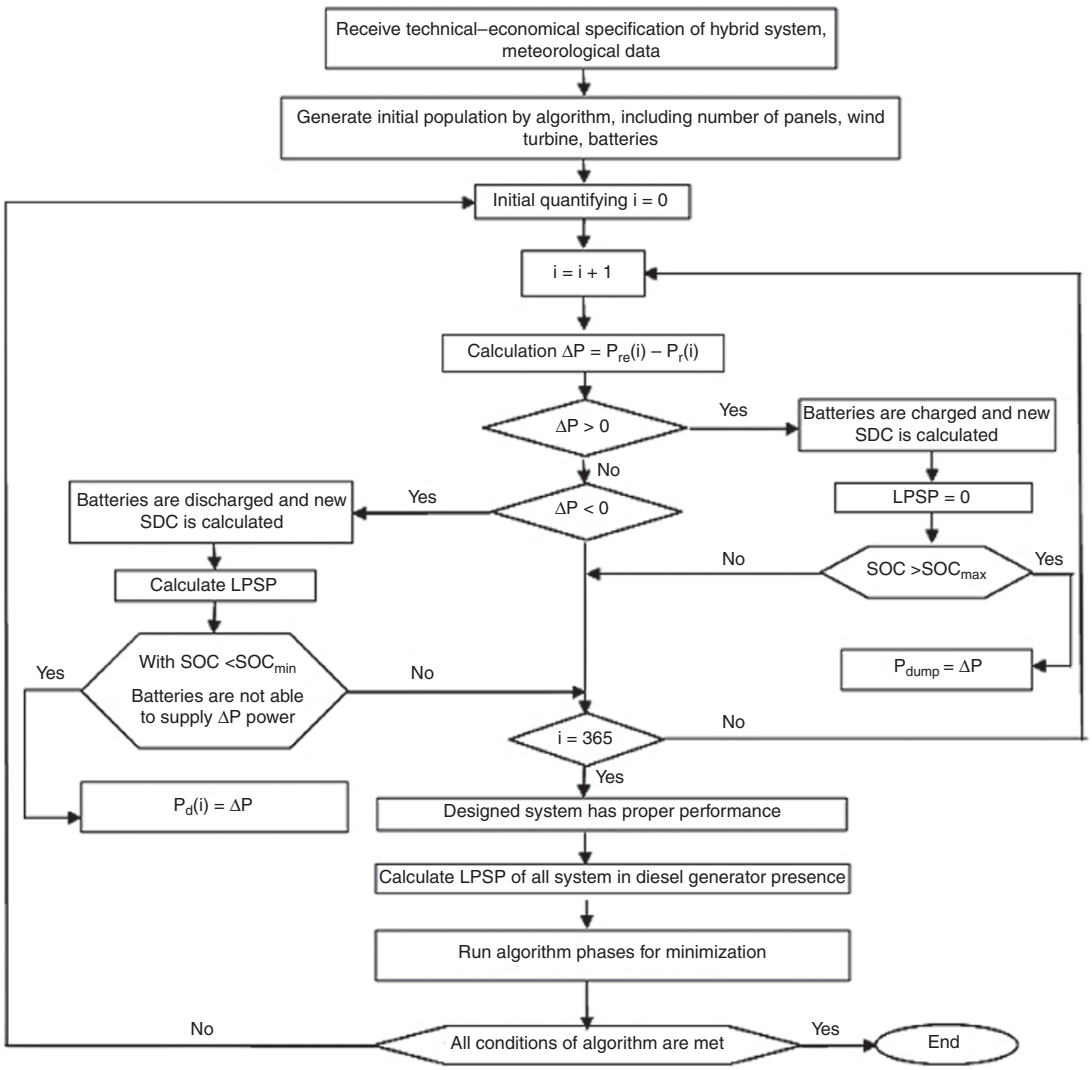

Fig. 7: Flowchart of the optimal design process of the proposed hybrid system using the colonial-competition algorithm [35].

1.1.4 *Diesel-generator model*

The total cost of the diesel generator is calculated as follows:

$$C_{T.D} = C_{I.D} + M_D + \frac{C_D}{Lief_D} + C_{fuel} \quad (15)$$

where $C_{I.D}$ is the installation cost ($), M_D is the hourly maintenance cost ($), C_D is the usage cost ($), $Lief_D$ is the lifetime in hours (h) and C_{fuel} is the fuel-consumption cost ($) of the diesel generator.

1.1.5 *Voltage inverter*

If the alternating current (AC) output is considered for the converter, e.g. if the energy of the photovoltaic converter is injected into the power grid, it is necessary to convert the direct current (DC) output voltage of the converter to AC using an electronic circuit, which can be single-phase or three-phase, depending on the application. The electronic circuit used to convert DC voltage to AC is called an inverter. The input DC voltage to the inverter in a photovoltaic power plant can be generated from the output of the solar arrays or the output of the battery used in the photovoltaic system.

The ground-phase voltage (V_{ph}) of the inverter output at the base frequency (60 or 50 Hz) is related to the DC input voltage to the inverter (V_d) as follows:

$$V_{ph} = \left(\frac{2.8}{\pi}\right) \cos\left(\frac{\pi}{6}\right) .V_d \quad (16)$$

The line-to-line voltage of the AC inverter output is 1/7 V_{ph}. In a steady state, the amount of DC power input to the inverter (P_{DC}) is equal to the sum of losses and the AC power of the inverter output (P_{AC}):

$$P_{DC} = \frac{P_{AC}}{\eta} \quad (17)$$

In the above relation, η represents the inverter efficiency.

1.2 Climatic profile of the study area

The geographical characteristics of the study area can be seen in Fig. 2. This region is located in the north-west of Iran. The amount of electrical charge required for this area can be seen in Fig. 3 at different times of the day.

A 12-month collection of information on wind speed, solar radiation and ambient temperature as a daily average recorded by the Meteorological Organization (http://www.satba.gov.ir/) can be seen in Figs 4–6. This information leads to more accurate and practical results. The wind speed has been recorded at an altitude of 40 m.

According to Fig. 4, in which the ambient temperature is observable, these data are used in modelling photovoltaic cells as the input in relationships to determine the actual efficiency. As shown in Fig. 6, the amount of solar-radiation intensity is used as the input in cell modelling so that the amount of power produced in a year is consistent with the amount of annual radiation intensity and a constant amount is not used.

Table 2: Techno-economic specifications of photovoltaic panels [36, 37]

Parameter	Amount
V_{OC} (V)	33.2
I_{SC} (A)	8.85
V_{max} (V)	26.6
I_{max} (A)	7.9
NCOT (°C)	47.9
Investment cost ($)	2000
Replacement cost ($)	2000
Maintenance and repairs ($/year)	10

Table 3: Techno-economic specifications of wind turbines [36, 37]

Parameter	Amount
Nominal power (kW)	5
υ_r (m/s)	11
υ_{ci} (m/s)	2.5
υ_{CO} (m/s)	24
Investment cost ($)	5000
Replacement cost ($)	4000
Maintenance and repairs ($/year)	75

Table 4: Techno-economic specifications of storage batteries [36, 37]

Parameter	Amount
Nominal capacity (Ah)	230
Nominal voltage (V)	12
Maximum discharge depth (%)	80
Efficiency (%)	85
Investment cost ($)	1200
Replacement cost ($)	1100
Maintenance and repairs ($/year)	50

The amount of wind that can be seen in Fig. 7 is used as an input of wind-turbine relations to calculate the production capacity of the wind turbine.

1.3 Specifications of the system equipment under study

The technical specifications of the individual pieces of the equipment used in modelling the studied system, including wind turbine, photovoltaic cell, diesel generator, battery and converter, can be seen in Tables 2–4 [36, 37].

In order to establish the connection between DC production and AC consumption, an electronic power converter is required. For the 4-kW system, the installation and replacement cost is estimated at $420. The sizes of 7, 8 and 9 kW are examined. The lifetime of the converters is 20 years and their efficiency is 85%. The cost of a commercial diesel generator available in the market may vary from 250 to 350 $/kW. For larger units, the price per kilowatt is lower than for smaller units. The price of a diesel generator in this analysis is considered equal to $300 and the cost of replacement and repair is assumed

to be 270 $/kW and 0.1 $/hr. Four different sizes with values 0, 2, 3 and 4 kW, respectively, are intended for diesel generators. To analyse the sensitivity of diesel fuel prices, four discrete values (0.5, 1.5, 2 and 2.5 $/l) were given to this variable. The fuel price is considered as 0.9 $/l.

1.4 Optimization

The ant-colony algorithm is inspired by studies and observations on ant colonies. One of the most important and interesting behaviours of ants is their behaviour to find food and especially how they find the shortest path between food sources and nests. One of the applications of this algorithm is to reach an almost optimal solution to the travelling-salesman problem. Thus, a variety of ant-colony algorithms have been developed to solve this problem [38, 39]. This numerical method has an advantage over analytical and genetic methods in cases in which the graph is constantly changing over time; and it is a reproducible algorithm so, over time, it responds to changes effectively.

According to Fig. 7, first, the meteorological data and techno-economic specifications of the equipment are obtained by the algorithm and the initial population is generated. For each population, the system performance cycle and power supply probability (LPSP) are calculated 365 times. If the obtained system has the correct performance, then the reliability is calculated for the whole hybrid system and the next steps of the algorithm are executed with the number of iterations to reach the lowest possible cost and the best combination.

1.4.1 *Objective function and problem constraints*

The objective function is the net present cost (NPC)(x) in dollars, which is equivalent to the sum of the total investment cost ($C_T(x)$), maintenance cost ($C_M(x)$), installation cost ($C_R(x)$) and total cost of the diesel generator in the service life of the system, assumed to be equivalent to 20 years of photovoltaic panels. The objective function for minimization is expressed as follows:

$$NPC\,(X) = N \times \{[CC + RC \times K\,(i_r, L, y) \times CRF\,(i_r, R) + C_M \quad (18)$$

where N is the number or capacity of the equipment, C_T is the initial investment cost, C_R is the cost of each installation y and L are the number of installations and the useful lifetime of the respective equipment, respectively, and C is the annual maintenance cost of the equipment. R is the lifetime of the project (20 years in this article) and i_r is the real interest (6% in this article), which can be calculated in terms of nominal interest ($i_{r\ nominal}$) and annual inflation rate (f_r) according to the following equation:

$$i_r = \frac{(i_{r,naminal} - f_r)}{1 + f_r} \quad (19)$$

CRF and K are the current values of the annual and fixed payments, respectively, which are defined as follows:

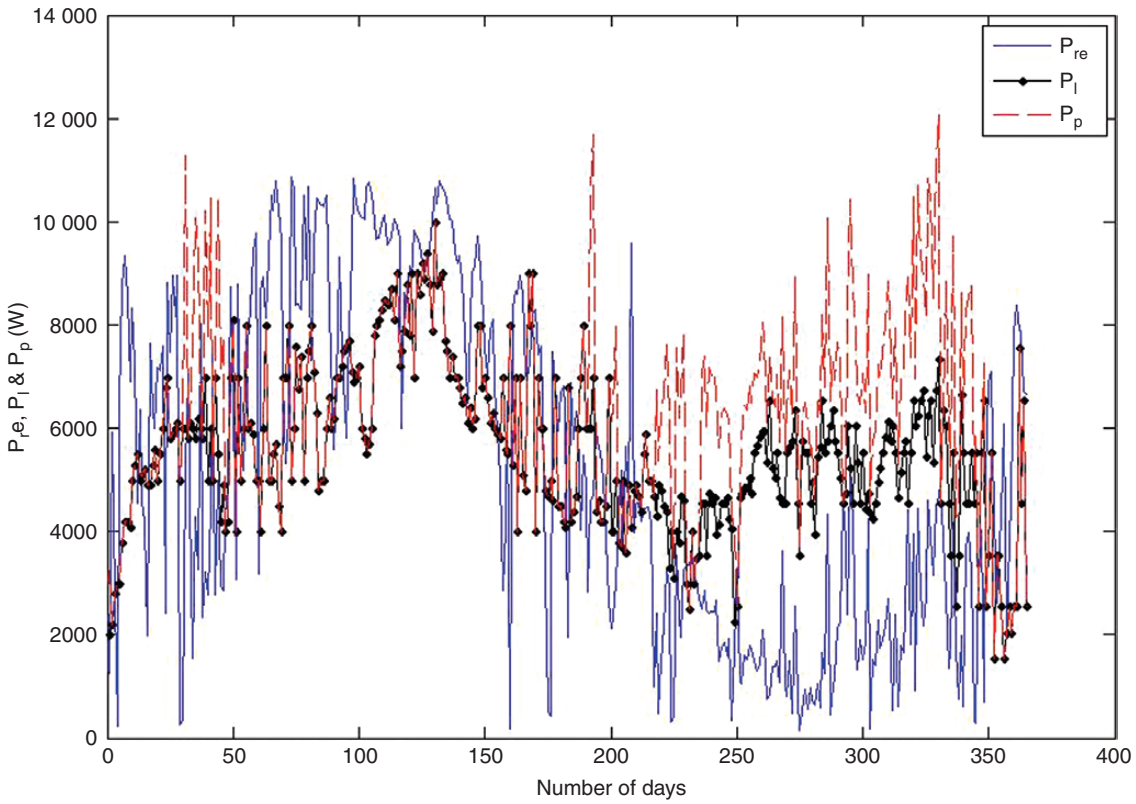

Fig. 8: Total production capacity (Pp), renewable-energy-production capacity (P_{re}) and load capacity (P_l) for the solar-diesel system.

$$CRF\left(i_R, R\right) = \frac{\left(1+i_r\right)^R - 1}{\left(1+i_r\right)^R i_r} \quad (20)$$

$$K_i = \sum_{n=1}^{y_i} \frac{1}{\left(1+i_r\right)^R} \quad (21)$$

2 Results

2.1 Modelling results

Figs 8–22 show how the load is supplied and the share of renewables, diesel generators and batteries in different scenarios of reliable load supply. The SOC of the batteries and reliability of the systems (LPSP) in all three combinations are also shown.

2.1.1 *Scenario 1: Photovoltaic cell–diesel generator hybrid system with battery storage for the hybrid*

Power and reliability diagrams for the solar–diesel system are shown in **Figs 8–12**.

Fig. 8 shows the generated power by renewable sources (P_{re}), the total generated power by the hybrid system (P_p) and the required load power in solar–diesel systems. The power produced by renewable sources in the studied system is 164 days more than the required power of the load and the additional power produced is spent on charging the batteries. Also, 201 days of renewable resources will not be able to supply the load, so the backup system will supply the load according to the mentioned strategy.

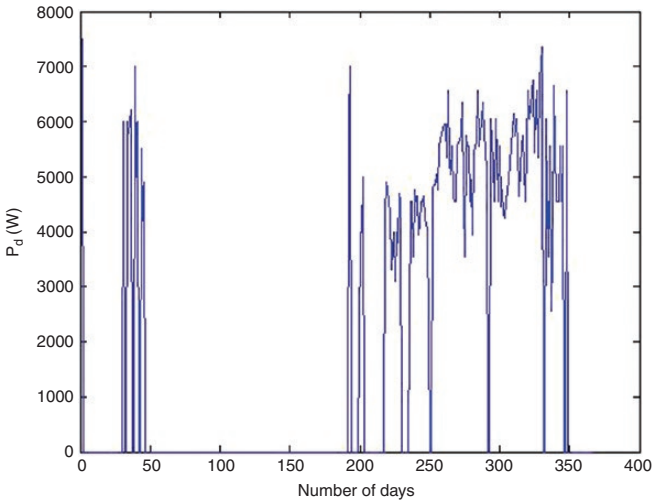

Fig. 10: Output power of the diesel generator during the year for the solar-diesel system.

Fig. 9 shows the input/output capacity of the battery bank and shows how they are charged and discharged throughout the year. $P_b > 0$ indicates the battery-charge and battery-input power, and $P_b > 0$ indicates the battery-discharge and battery-output power. This figure is related to the solar–diesel system. Due to this shape, the batteries in the system under study are charged for 164 days. The batteries also discharge for 68 days and supply the load. Finally, the length of time that the batteries are neither charged nor discharged during the day for the system under study is 133 days.

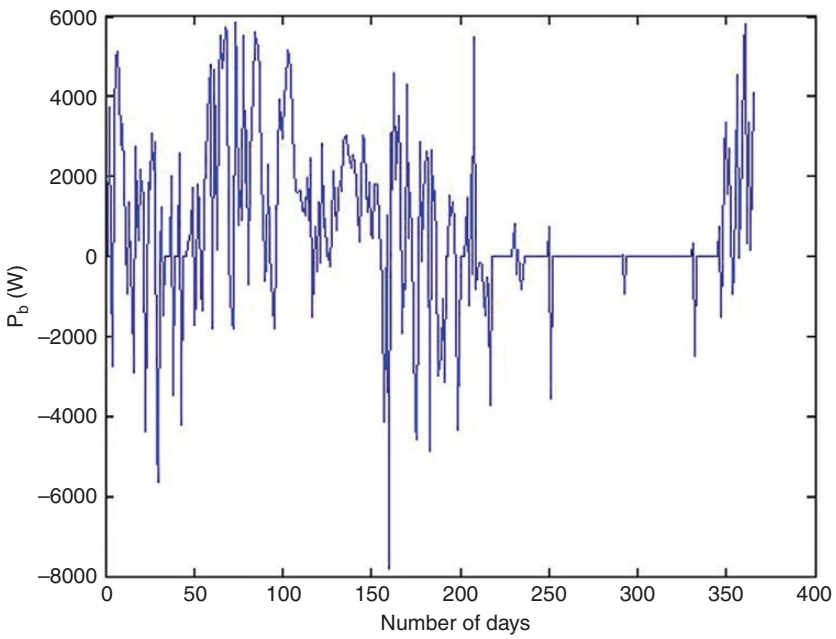

Fig. 9: Input/output power of the battery bank during the year for the solar-diesel system.

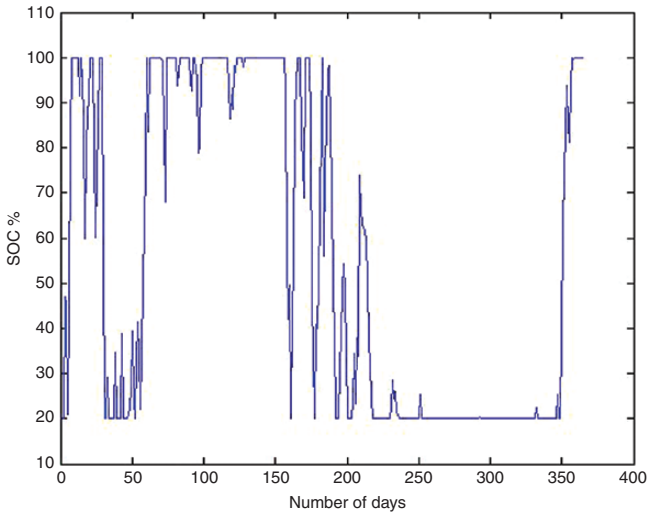

Fig. 11: SOC of the battery bank during the year for the solar-diesel system.

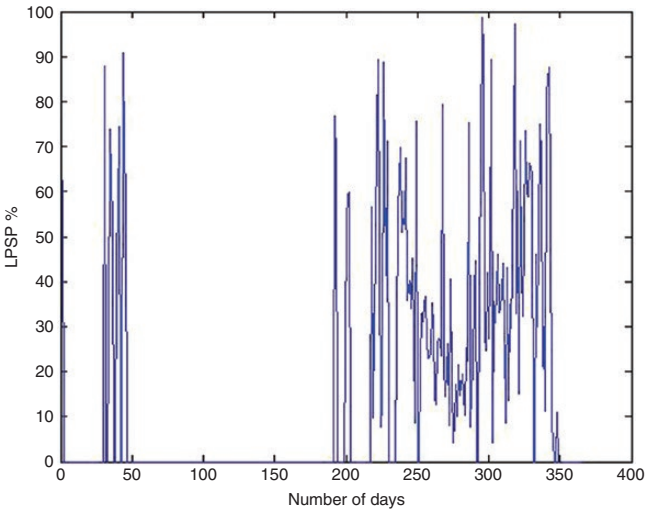

Fig. 12: System reliability during the year for the solar-diesel system.

Fig. 10 shows how the diesel generator works throughout the year. In this design, the diesel generator supplies the load when the used renewable sources and the battery bank are not able to supply the required load power. According to the figure, it can be observed that the diesel generator does not work at its nominal power on any day of the year. Its maximum output power is 7.5 kW for 1 day of the year for the solar–diesel hybrid system. Also, for 232 days for the hybrid solar–diesel system, the output power of the diesel generator is 0, which indicates fuel savings. The cost of the annual fuel consumption in this system is $2398, which, if the diesel system is used instead of these systems, will result in a fuel cost of $22 234.

Fig. 11 shows the SOC pointer of the battery and it can be observed that the SOC of the battery bank for all three hybrid systems studied is between SOC_{msx} (100% SOC) and SOC_{min} (20% SOC), which shows the correct operation of the designed systems.

Fig. 12 shows the reliability indicator of the hybrid solar–diesel system throughout the year. If the LPSP is 0, the load will be reliably supplied by the designed system and if the LPSP is 1, the designed system will not be able to supply the load. It can be observed that the desired 10-kW load is fully supported by the designed solar–diesel system.

2.1.2 *Scenario 2: Wind–diesel generator turbine system with battery storage*

For the optimal wind–diesel system, the power and reliability diagrams are as follows. Fig. 13 shows the power generated by renewable sources (*Pre*), the total power generated by the wind–diesel hybrid system (*Pp*) and the load power required in the wind–diesel system. The power produced by renewable sources in the system under study is 128 days more than the required power of the load; the additional power generated is spent on

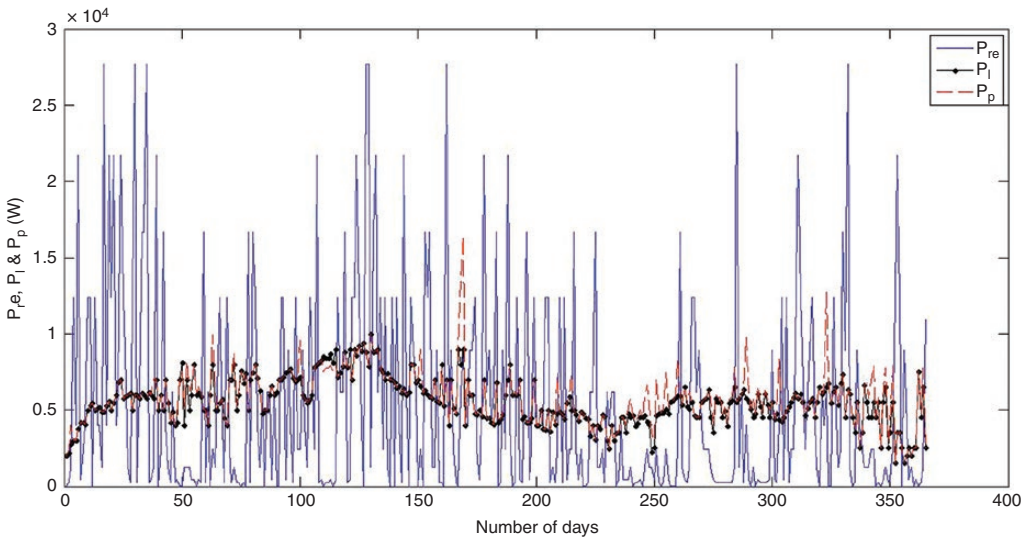

Fig. 13: Total production capacity (*Pp*), renewable-energy-production capacity (P_{re}) and load capacity (P_l) for the wind-diesel system.

charging the batteries. Also, 237 days of renewable resources will not be able to supply the load, so the backup system will supply the load according to the mentioned strategy.

Fig. 14 shows the input/output capacity of the battery bank for the wind–diesel system and shows how they are charged and discharged throughout the year. $P_b > 0$ indicates the battery-charge and battery-input power, and $P_b < 0$ indicates the battery-discharge and battery-output power. According to this diagram, the batteries in the studied air–diesel system are charged for 128 days. The batteries also discharge for 125 days and supply the load. Finally, the length of time for which batteries are neither charged nor discharged during the day for the wind–diesel system is 112 days.

Fig. 15 shows how the diesel generator works throughout the year. According to the figure, it can be seen that the diesel generator does not work at its nominal power on any day of the year. Its maximum output power is in the hybrid 7.5 kW for 16 days of the year for the hybrid wind–diesel system. Also, for 237 days for the hybrid wind–diesel system, the output power of the diesel generator is 0, which indicates fuel savings. The annual fuel-consumption cost of these systems is $2270, which, if the diesel system is used instead, will result in a fuel-consumption cost of $22 234.

Fig. 16 shows the SOC of the battery and shows that the SOC of the battery bank for the studied hybrid system is between SOC_{max} (100% SOC) and SOC_{min} (20% SOC), which shows the correct operation of the designed system. Fig.

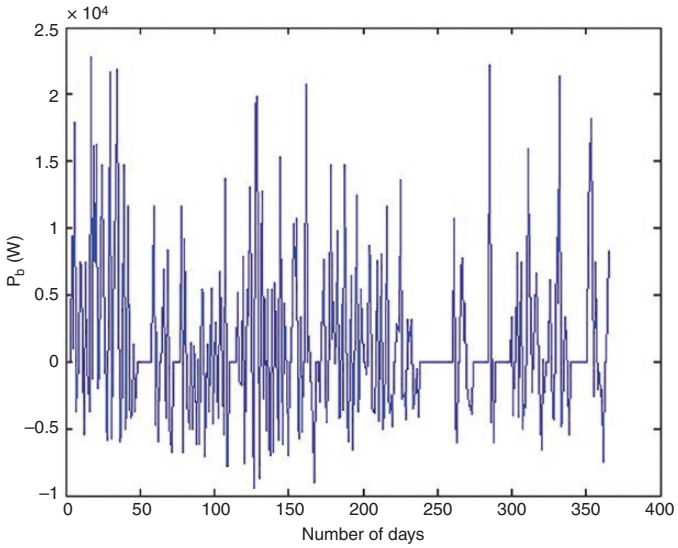

Fig. 14: Input/output power of the battery bank during 1 year for the wind-diesel system.

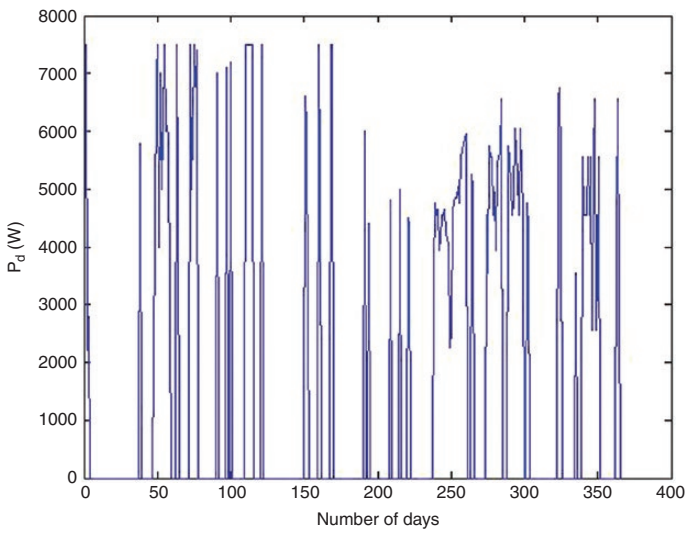

Fig. 15: Output power of the diesel generator during the year for the wind-diesel system.

17 shows the reliability index of the hybrid wind–diesel system throughout the year. If the LPSP is 0, the load will be reliably supplied by the designed system and, if the LPSP is 100%, the designed system will not be able to supply the load.

It can be seen that the desired 10-kW load is fully supported by the designed wind–diesel system.

2.1.3 *Scenario 3: Photovoltaic cell–wind turbine–diesel generator systems with battery storage*

Finally, the power and reliability diagrams for the optimal hybrid solar–wind–diesel system shown in Figs 18–22. Fig. 18 shows the power generated by renewable sources (P_{re}), the total power generated by the hybrid system (P_p) and the required load power of the wind–diesel solar system. The power produced by renewable sources in the studied

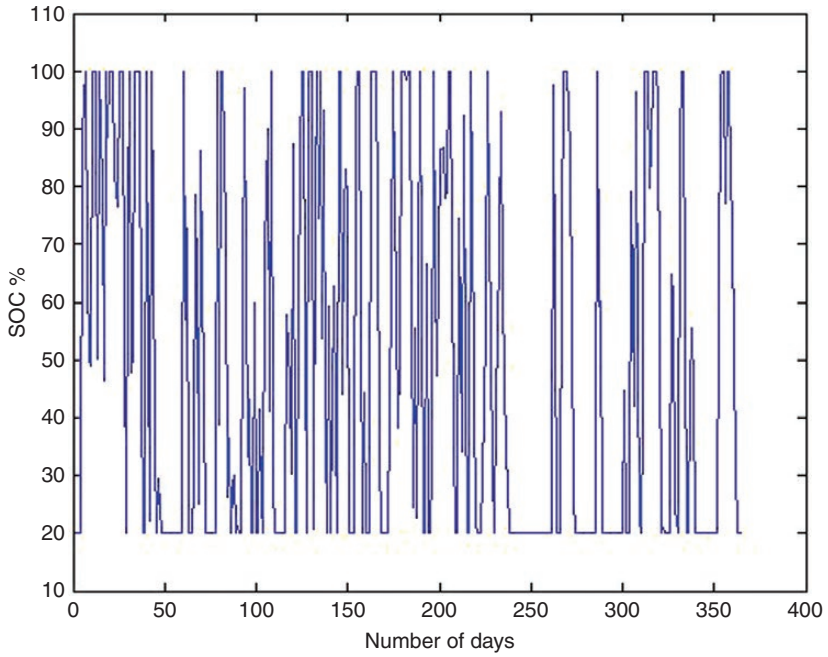

Fig. 16: SOC of the battery bank during the year for the wind-diesel system.

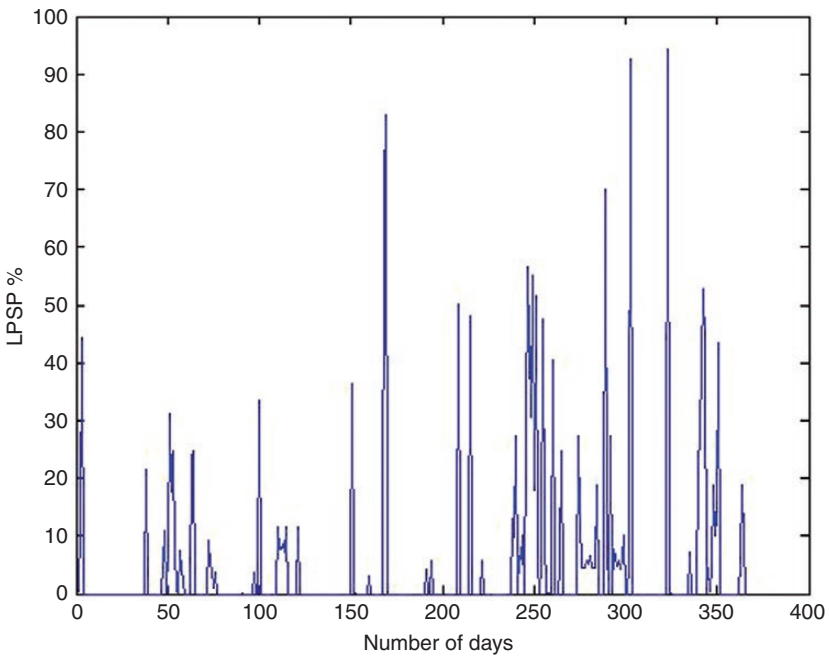

Fig. 17: Reliability of the system during the year for the wind-diesel system.

system is 137 days more than the required power of the load; the additional power generated is spent on charging the batteries. Two hundred and twenty-eight days of renewable resources will not be able to supply the load, so the backup system will supply the load according to the mentioned strategy. Fig. 19 shows the input/output power of the battery bank during the year.

Fig. 19 shows the input/output power of the battery bank in the optimal solar-wind–diesel system and shows how they are charged and discharged throughout the year. $P_b > 0$ indicates the battery-charge and battery-input power, and $P_b < 0$ indicates the battery-discharge and battery-output power. Due to this shape, the batteries in the studied system are charged for 137 days. The batteries are also discharged for 121 days and supply the load. Finally, the length of time for which the batteries are neither charged nor discharged during the day is 107 days for the system under study. Fig. 20 shows the input/output power of the diesel generator during the year.

Fig. 20 shows how a diesel generator works throughout the year. It should be noted that the diesel generator does not

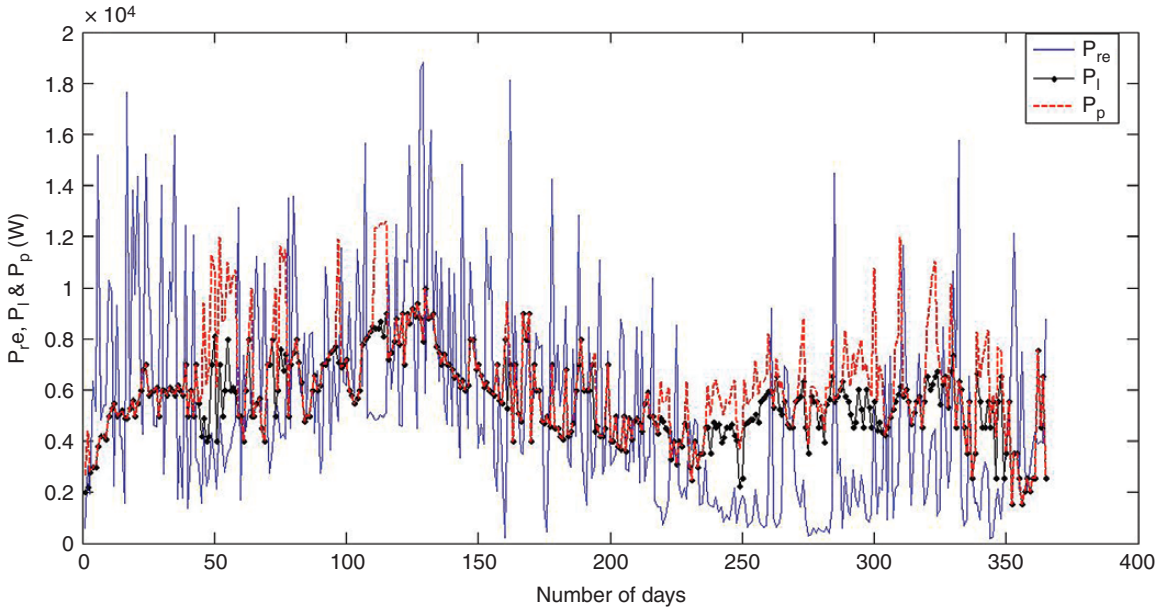

Fig. 18: Total production capacity (*Pp*), renewable-energy-production capacity (P_{re}) and load power (P_l) for the solar-wind-diesel system.

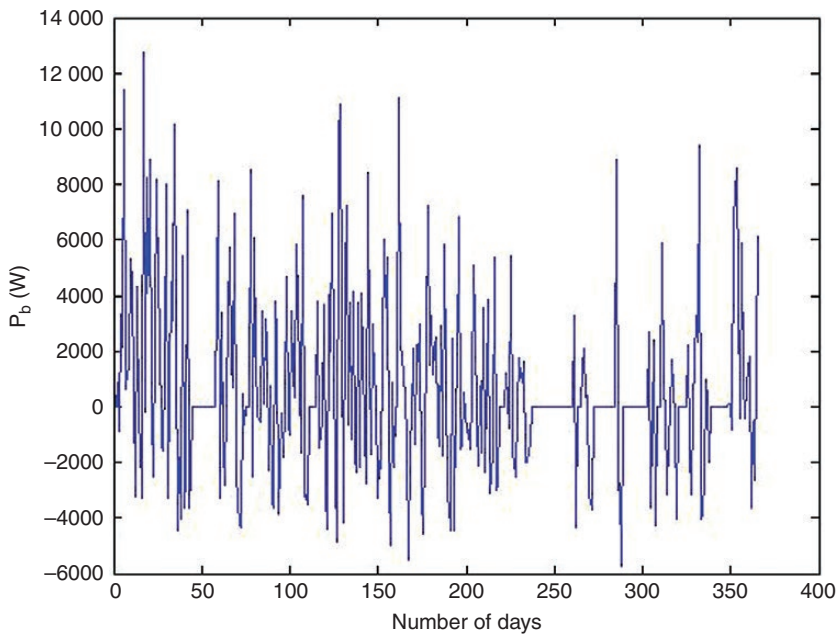

Fig. 19: Input/output power of the battery bank during the year for the solar-wind-diesel system.

operate at full capacity on any day of the year. Its maximum output power in all three hybrid systems is 7.5 kW per 10 days of the year for the hybrid solar–wind–diesel system. Also, for 244 days for the hybrid solar–wind–diesel system, the output power of the diesel generator is 0, which indicates a saving in fuel consumption. The annual fuel-consumption cost in these systems is $2144, which, if the diesel system is used instead of these systems, will result in a $22 234 fuel-consumption cost. Fig. 21 shows the SOC of the battery bank seen during the year.

Fig. 21 shows the SOC of the battery and it can be seen that the SOC of the battery bank for the studied system between SOC_{msx} (100% SOC) and SOC_{min} (20% SOC) shows the correct operation of the designed systems.

Fig. 22 shows the reliability indicators of the hybrid solar–wind–diesel system throughout the year. If the LPSP is 0, the load will be reliably supplied by the designed system and, if the LPSP is 100%, the designed system will not be able to supply the load. According to the above diagrams, it can be seen that the desired load of 10 kW is fully

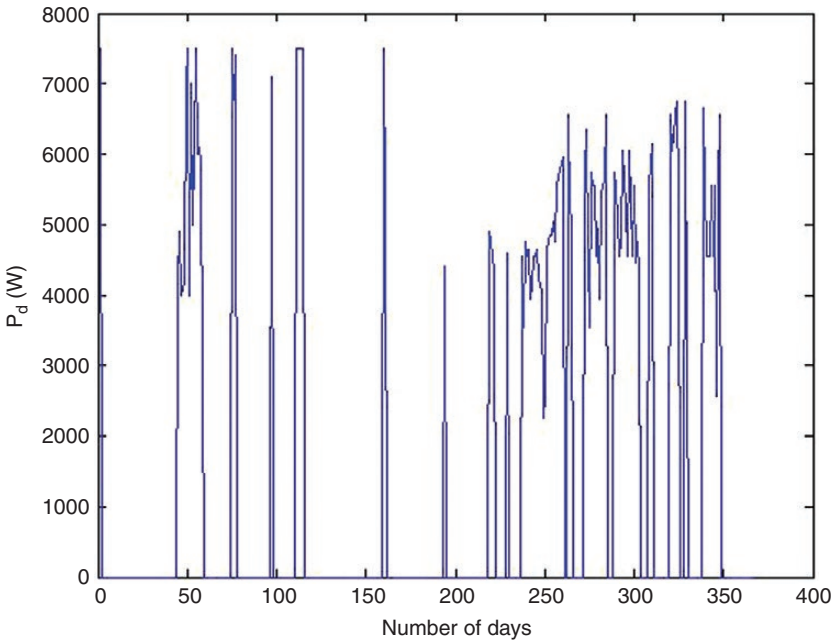

Fig. 20: Output power of the diesel generator during the year for the solar-wind-diesel system.

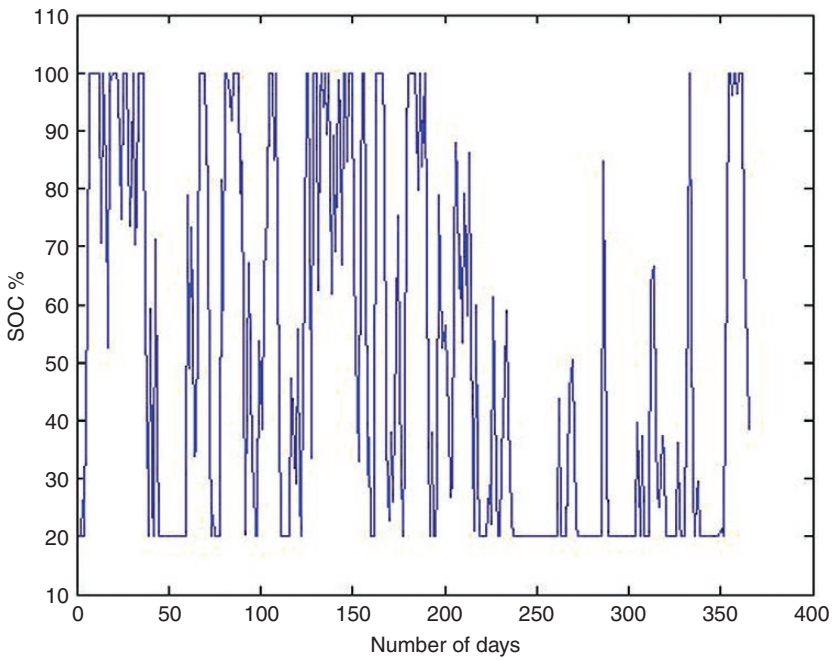

Fig. 21: SOC of the battery bank during the year for the solar-wind-diesel system.

supported by all three designed systems. And the way of support is also quite clear. In other words, wherever the battery and renewable sources cannot supply the load, the diesel generator immediately enters into operation and supplies the load.

2.2 Optimization results

The results of the optimal design of different hybrid systems with the total cost of the system obtained from the colonial-competition algorithm are shown in Table 5.

Finally, Fig. 23 shows the cost of different types of systems with diesel generators.

According to Fig. 23 and Table 5, it can be seen that combining renewable wind and solar sources with diesel generators is more profitable than combining wind or solar sources alone with diesel generators. In order to achieve the best answer and the lowest cost, the results of the colonial-competition algorithm are compared with the results of the genetic algorithms and particle-assembly optimization (PSO). For this purpose, the initial population is 30–100 repetitions. The results are shown in Fig. 24.

Considering Fig. 24, it can be seen that the costs of a hybrid solar–wind–diesel energy system during 20 years of system operation using colonial-competition algorithms, particle-assembly optimization and genetic algorithm (GA) are $71 498, $75 920 and $76 167, respectively. Among these algorithms, the evolutionary algorithm of colonial competition has a higher accuracy and speed than other algorithms used and gives a more reliable design. Considering Fig. 24, this algorithm converges from iteration 20, while particle-assembly and genetic-optimization algorithms converge from iterations 52 and 71, respectively. Table 6 also shows the optimal combinations of a solar–wind–diesel system using the proposed algorithms.

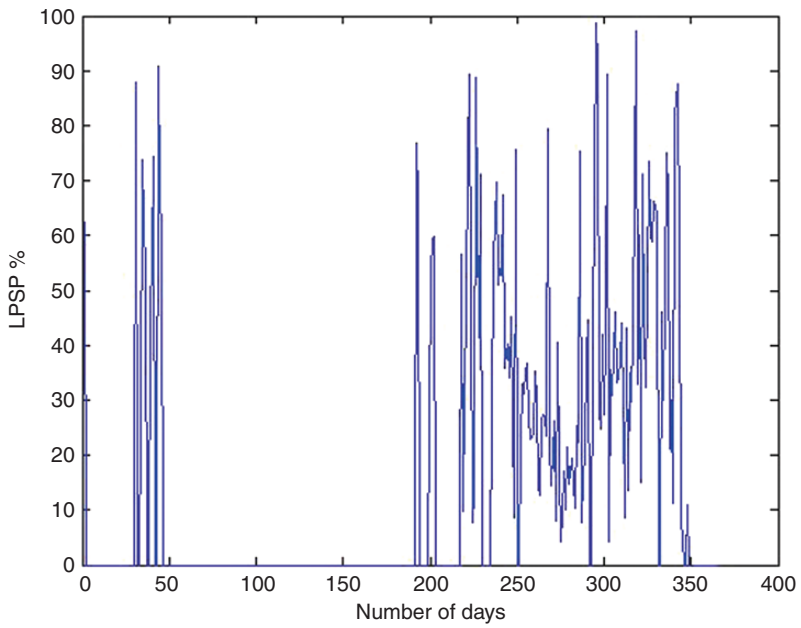

Fig. 22: System reliability during the year for the solar-wind-diesel system.

Table 5: Results of optimal design of different hybrid systems in the colonial-competition algorithm

	Type of hybrid system		
Optimal values	Solar–diesel	Wind–diesel	wind–solar–diesel
N_{PV}	67	0	33
N_{WT}	0	6	3
N_{Bat}	16	16	16
N_{inv}	9	9	9
LPSP	0.0691	0.0539	0.0684
Fuel-consumption cost in a year ($)	2398	2270	2144
Total construction cost ($)	106 135	93 857	71 498

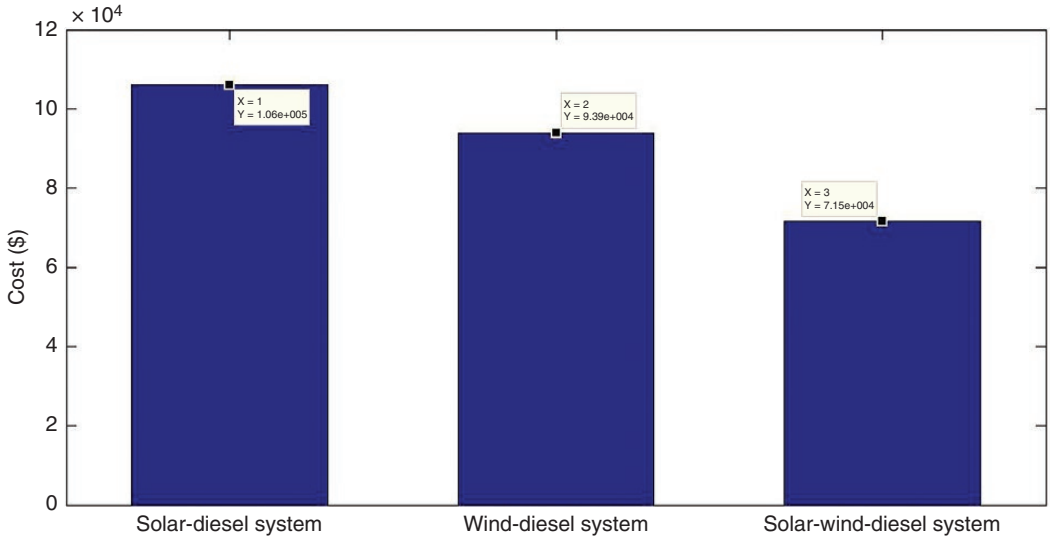

Fig. 23: Total cost of wind–diesel, solar–diesel and wind–solar–diesel systems in the proposed algorithm.

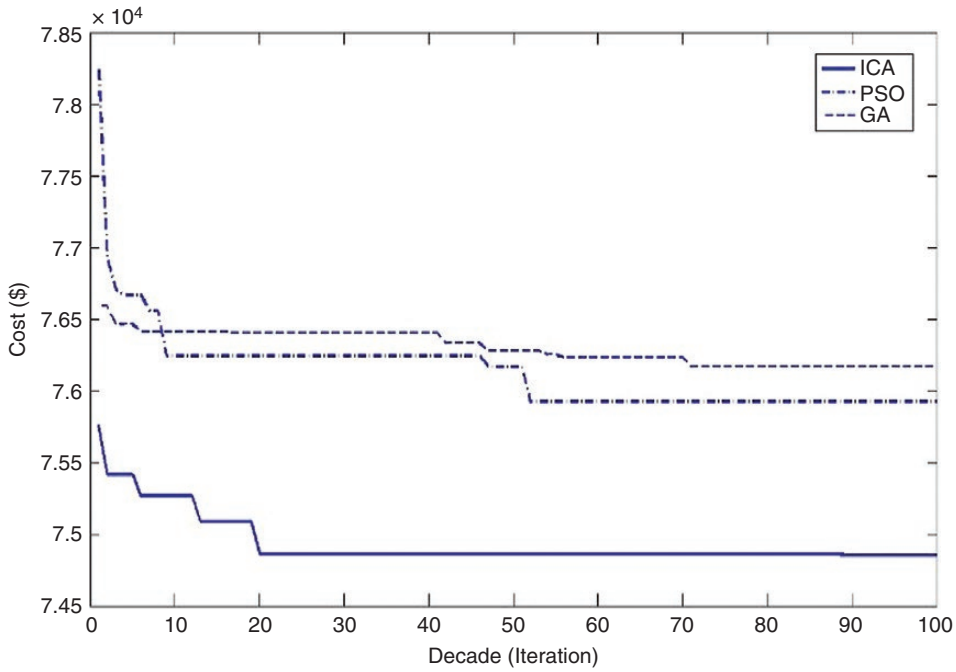

Fig. 24: Cost-convergence trend of hybrid wind–solar–diesel systems in colonial-competition algorithms, PSO and GA (research output).

Table 6: Total cost of the optimal hybrid system in optimization algorithms (research output)

	Optimization algorithm		
Parameter	ICA	PSO	GA
Total cost ($)	71 498	75 920	76 170

3 Conclusion

The use of renewable energy has become inevitable. But in this way, problems such as discontinuity and high investment costs and, by its nature, high return on investment have slowed down the use of these technologies. Most countries that use fossil-fuel sources are not so interested in importing these technologies into their country. But on the other hand, when using fossil fuels, pollutant gases are released into the atmosphere, which can be very dangerous for the future of the planet. In this research, an attempt has been made to address the need to use renewable-energy-based technologies by providing appropriate solutions in terms of economics and reliability. In the present study, different scenarios have been mentioned to provide the maximum required electric charge and, in terms of economic parameters and high reliability, the wind-turbine

system with a photovoltaic cell using diesel-generator support with battery energy storage was selected. The selected system has been optimized for better evaluation using the colonial-competition algorithm in order to reduce the cost of investment, maintenance and replacement by obtaining the appropriate size of equipment. Finally, in order to ensure the values obtained from optimization, the colonial-competition algorithm was evaluated in terms of the convergence process and determining the total investment cost using a genetic algorithm and PSO. One of the important results of this research is to provide the maximum load required by the selected system with lower costs than other scenarios and, on the other hand, the investment cost determined using the colonial-competition algorithm is lower than those using other algorithms.

Conflict of interest statement

There is no conflict of interest.

References

[1] Eriksson ELV, Gray EM. Optimization of renewable hybrid energy systems—a multi-objective approach. *Renewable Energy*, 2019, 133:971–999.

[2] Alayi R, Ahmadi MH, Visei AR, *et al*. Technical and environmental analysis of photovoltaic and solar water heater cogeneration system: a case study of Saveh City. *International Journal of Low-Carbon Technologies*, 2021, 16:447–453.

[3] Khalili H, Arash A, Alayi R. Simulation and economical optimization hybrid system PV and grid in Ardabil city. *Journal of Current Research in Science*, 2015, 3:83.

[4] Talha M, Sohail M, Tariq R, *et al*. Impact of oil prices, energy consumption and economic growth on the inflation rate in Malaysia. *Cuadernos de Economía*, 2021, 44:26–32.

[5] Alayi R, Jahanbin F. Generation management analysis of a stand-alone photovoltaic system with battery. *Renewable Energy Research and Application*, 2020, 1:205–209.

[6] Ehyaei MA, Assad MEH. Energy and exergy analyses of wind turbines. In: Assad MEH, Rosen MA (eds). Design and Performance Optimization of Renewable Energy Systems. Oxford, UK: Academic Press, 2021, 195–203. https://www.sciencedirect.com/science/article/pii/B9780128216026000158

[7] Sibuea MB, Sibuea SR, Pratama I. The impact of renewable energy and economic development on environmental quality of ASEAN countries. 2021, 23:12–21.

[8] Alayi R, Kumar R, Seydnouri SR, *et al*. Energy, environment and economic analyses of a parabolic trough concentrating photovoltaic/thermal system. *International Journal of Low-Carbon Technologies*, 2021, 16:570–576.

[9] Koohi-Fayegh S, Rosen MA. A review of renewable energy options, applications, facilitating technologies and recent developments. *European Journal of Sustainable Development Research*, 2020,4:em0138.

[10] Tun MM. An overview of renewable energy sources and their energy potential for sustainable development in Myanmar. *European Journal of Sustainable Development Research*, 2019, 3:em0071.

[11] Alayi R, Velayti J. Modeling/optimization and effect of environmental variables on energy production based on PV/Wind turbine hybrid system. *Jurnal Ilmiah Teknik Elektro Komputer dan Informatika (JITEKI)*, 2021, 7:101–107.

[12] Elavarasan RM. The motivation for renewable energy and its comparison with other energy sources: a review. *European Journal of Sustainable Development Research,* 2019, 3:em0076.

[13] Alayi R, Rouhi H. Techno-economic analysis of electrical energy generation from urban waste in Hamadan, Iran. *International Journal of Design & Nature and Ecodynamics*, 2020, 15:337–341.

[14] Kool ED, Cuomo MA, Reddy BV, *et al*. Multi-generation renewable energy system for dairy farms: exergy analysis. *European Journal of Sustainable Development Research*, 2018, 2:37.

[15] Kasaeian A, Shamel A, Alayi R. Simulation and economic optimization of wind turbines and photovoltaic hybrid system with storage battery and hydrogen tank. *Journal of Current Research in Science*, 2015, 3:105.

[16] Shamel A, Marefati M, Alayi R, *et al*. Designing a PID controller to control a fuel cell voltage using the imperialist competitive algorithm. *Advances in Science and Technology. Research Journal*, 2016, 10:176—181.

[17] Barakat S, Ibrahim H, Elbaset AA. Multi-objective optimization of grid-connected PV-wind hybrid system considering reliability, cost, and environmental aspects. *Sustainable Cities and Society*, 2020, 60:102178.

[18] Alayi R, Khan MRB, Mohmammadi MSG. Feasibility study of grid-connected PV system for peak demand reduction of a residential building in Tehran, Iran. *Mathematical Modelling of Engineering Problems*, 2020, 7:563–567.

[19] Wang R, Xiong J, He MF, *et al*. Multi-objective optimal design of hybrid renewable energy system under multiple scenarios. *Renewable Energy*, 2020, 151:226–237.

[20] Yang Y, Li R. Techno-economic optimization of an off-grid solar/wind/battery hybrid system with a novel multi-objective differential evolution algorithm. *Energies*, 2020, 13:1585.

[21] Ibrahim IA, Sabah S, Abbas R, *et al*. A novel sizing method of a standalone photovoltaic system for powering a mobile network base station using a multi-objective wind driven optimization algorithm. *Energy Conversion and Management*, 2021, 238:114179.

[22] Alayi R, Kasaeian A, Najafi A. *et al*. Optimization and evaluation of a wind, solar and fuel cell hybrid system in supplying electricity to a remote district in national grid. *International Journal of Energy Sector Management*, 2020, 14:408–418.

[23] Ridha HM, Gomes C, Hizam H, *et al*. Multi-objective optimization and multi-criteria decision-making methods for optimal design of standalone photovoltaic system: a comprehensive review. *Renewable and Sustainable Energy Reviews*, 2021, 135:110202.

[24] Shivam K, Tzou JC, Wu SC. A multi-objective predictive energy management strategy for residential grid-connected PV-battery hybrid systems based on machine learning technique. *Energy Conversion and Management*, 2021, 237:114103.

[25] Hysa A. Modeling and simulation of the photovoltaic cells for different values of physical and environmental parameters. *Emerging Science Journal*, 2019, 3:395–406.

[26] Abbassi R, Abbassi A, Heidari AA, *et al*. An efficient salp swarm-inspired algorithm for parameters identification of photovoltaic cell models. *Energy Conversion and Management*, 2019, 179:362–372.

[27] Shukla A, Khare M, Shukla KN. Modeling and simulation of solar PV module on MATLAB/Simulink. *Engineering and Technology*, 2015, 4:3297.

[28] Bouaziz N, Benfdila A, Lakhlef A. A model for predicting photovoltaic module performances. *International Journal of Power Electronics and Drive Systems*, 2019, 10:1914.

[29] Alvarez DI, Calle Castro CJ, Gonzalez FC, *et al*. Modeling and simulation of a hybrid system solar panel and wind turbine in the locality of Molleturo in Ecuador. In:2017 IEEE 6th International Conference on Renewable Energy Research and

Applications (ICRERA), San Diego, CA, 5–8 November 2017, 620–625.

[30] Karamichailidou D, Kaloutsa V, Alexandridis A. Wind turbine power curve modeling using radial basis function neural networks and tabu search. *Renewable Energy,* 2021, 163:2137–2152.

[31] Fazlollahi V, Taghizadeh M, Ayatollah zade Shirazi F. Modeling and neuro-fuzzy controller design of a wind turbine in full-load region based on operational data. *AUT Journal of Modeling and Simulation*, 2019, 51:139–152.

[32] Manobel B, Sehnke F, Lazzús JA, *et al*. Wind turbine power curve modeling based on Gaussian processes and artificial neural networks. *Renewable Energy,* 2018, 125:1015–1020.

[33] Yang N, Fu Y, Yue H, *et al*. An improved semi-empirical model for thermal analysis of lithium-ion batteries. *Electrochimica Acta*, 2019, 311:8–20.

[34] Cui Z, Poblete FR, Zhu Y. Tailoring the temperature coefficient of resistance of silver nanowire nanocomposites and their application as stretchable temperature sensors. *ACS Applied Materials & Interfaces*, 2019, 11:17836–17842.

[35] Khalilnejad A, Sundararajan A, Sarwat A. I Optimal design of hybrid wind/photovoltaic electrolyzer for maximum hydrogen production using imperialist competitive algorithm. *Journal of Modern Power Systems and Clean Energy*, 2018, 6:40–49.

[36] Moein M, Pahlavan S, Jahangiri M, *et al*. Finding the minimum distance from the national electricity grid for the cost-effective use of diesel generator-based hybrid renewable systems in Iran. *Journal of Renewable Energy and Environment*, 2018, 5:8–22.

[37] Mostafaeipour A, Jahangiri M, Haghani A, *et al*. Statistical evaluation of using the new generation of wind turbines in South Africa. *Energy Reports*, 2020, 6:2816–2827.

[38] Karaboga D. Artificial bee colony algorithm. *Scholarpedia*, 2010, 5:6915.

[39] Gao WF, Liu SY. A modified artificial bee colony algorithm. *Computers & Operations Research*, 2012, 39:687–697.